Journal of Organometallic Chemistry, 238 (1982) 267—279
Elsevier Sequoia S.A., Lausanne — Printed in The Netherlands

FLUORINE SUBSTITUTION EFFECTS IN ORGANOBORATE CHEMISTRY: VIBRATIONAL AND X-RAY STRUCTURAL ANALYSES OF $K[CH_3BF_3]$

D.J. BRAUER, H. BÜRGER * and G. PAWELKE

Anorganische Chemie, FB 9, Universität-Gesamthochschule D-5600, Wuppertal, (F.R.G.)

(Received May 17th, 1982)

Summary

The IR and Raman spectra of ^{10}B and ^{11}B $K[CH_3BF_3]$ and $K[CD_3{}^{11}BF_3]$ are reported, assigned and used to determine a quadratic force field for the anion. The crystal structure (*Pbca*, *a* 17.172(2), *b* 7.1486(9), *c* 7.2289(7) Å, $Z = 8$, d_c 1.825 g/cm^3) has been determined from 933 X-ray data and refined to a conventional R value of 0.026. Anion symmetry deviates only slightly from C_{3v} in the solid state. Values derived for the B—C (1.575(3) Å) and mean B—F (1.424(5) Å) bond lengths are the shortest and longest, respectively, found to date in borate structures. The corresponding force constants are f(BC) 3.7 and f(BF) 3.96 × 10^2 N m^{-1}. The F—B—F and C—B—F bond angles average 105.4(5) and 113.3(4)°, respectively. Seven K—F contacts (2.678(1)—2.965(1) Å) are the principal cation-anion interactions in the crystal.

Introduction

Bonds between CF_3 groups and electropositive elements such as Ge [1], Sn [2], As [3] and Hg [4,5,6] have been found to be longer and to possess smaller force constants than those in the relevant CH_3 analogs. Explanations for this unusual but systematic substitution effect have focussed on a reduction of the ionic bond character in CF_3 derivatives of such electropositive elements [2,7]. However, this trend has not been confirmed for boron compounds due to a lack of investigations on species of exact comparability. Structural and vibrational spectroscopic investigations of $K[CF_3BF_3]$ [8] and $Cs[(CF_3)_2BF_2]$ [9] have, however, shown that the B—C bond lengths and force constants correspond to those in the $B(CH_3)_4^-$ anion [10,11].

In addition, substitution of a F ligand in $CF_3BF_3^-$ by a CF_3 group causes no detectable changes in the B—CF_3 bond parameters [9]. Whether the B—CH_3 bonds in $B(CH_3)_4^-$ are equally insensitive to F/CH_3 substitution is by no means obvious. To clarify this point and thus provide a firm basis for a discussion of

0022-328X/82/0000—0000/$02.75

the CF_3/CH_3 substitution effect in borate chemistry, we have carried out a X-ray structural and vibrational analysis of $K[CH_3BF_3]$. For the spectroscopic study, the isotopic species $K[CD_3BF_3]$ and $K[CH_3{}^{10}BF_3]$ were also prepared.

Experimental

Synthesis

$K[CH_3BF_3]$ was prepared from CH_3BF_2 [12] and aqueous KF by Stafford's procedure [13]. For $K[CD_3BF_3]$ and $K[CH_3{}^{10}BF_3]$, CD_3BF_2 and $CH_3{}^{10}BF_2$ were synthesized from $Sn(CD_3)_4$ and BF_3 or $Sn(CH_3)_4$ and $^{10}BF_3$ (from Oak Ridge $^{10}B_2O_3$, 92.4%), respectively.

Spectra

Raman spectra were obtained from single crystals and powders employing a Cary 82 spectrometer and Kr^+ 6471 Å excitation, 200 mW at the sample, wave number accuracy 1—2 cm^{-1}. IR spectra of KBr and CsBr pellets in the 4000 to 180 cm^{-1} frequency range were recorded with a Perkin—Elmer 580 B grating spectrometer, wave number accuracy 1—2 cm^{-1}.

X-ray analysis

Crystals of $K[CH_3BF_3]$ were grown by slow evaporation of a $CH_3OH/CH_3OCH_2CH_2OCH_3$ solution in a desiccator over P_4O_{10}, cleaved and glued to a thin glass fiber. The orthorhombic space group was determined from the symmetry and systematic absences revealed by precession and Weissenberg photographs.

TABLE 1

CRYSTAL DATA FOR $K[CH_3BF_3]$

Crystal system	orthorhombic
a	17.172(2) Å [a]
b	7.1486(9) Å
c	7.2289(7) Å
Z	8
d_c	1.825 g cm^{-3}
T	20° C
Systematic absences	$hk0$ $h = 2n + 1$
	$h0l$ $l = 2n + 1$
	$0kl$ $k = 2n + 1$
Space group	$Pbca$
Octants measured	hkl, $\bar{h}kl$ (partial)
λ	0.71069 Å (Mo-$K_{\bar{\alpha}}$)
Monochromator	graphite
Maximum θ	30°
Scan technique	$\omega - 2\theta$
Scan width (ω)	1.00° + 0.35° tan θ
Scan speed (2θ)	1.11—10.00° min^{-1}
Reflections measured	1864
Unique (minus absences)	1269
With $\|F_0\| \geq 4\sigma(\|F_0\|)$	933
Weights w	$[\sigma^2(\|F_0\|) + 0.0004\|F_0\|^2]^{-1}$
Crystal size	0.16 × 0.406 × 0.492 mm
μ(Mo-K_α)	11 cm^{-1}
Transmission factors	0.640—0.838

[a] Numbers in parentheses in this manuscript represent estimated standard deviations in the last digit.

Further measurements were made with a CAD-4 diffractometer. The sharp and symmetric ω profiles of three strong, low order reflections proved the suitability of the crystal for an X-ray examination.

Intensity data were collected by the ω-2θ scan technique. During the measurement, the intensities of three periodically monitored standard reflections varied less than ±4%. Then 75 reflections were centered, and these Bragg angles were used to calculate the precise cell constants. ψ-scans of 18 reflections were collected and used later to check the validity of the numerical absorption correction. Crystal data and details of the intensity measurement are included in Table 1.

Intensities were calculated, corrected for monitor reflection fluctuations, and converted to $|F_o|$'s. These were assigned weights $w = (\sigma^2(|F_o|) + 0.0004\ |F_o|^2)^{-1}$. Only those reflections with $|F_o| \geq 4\sigma(|F_o|)$ were deemed observed and used in the solution and refinement of the structure.

The structure was solved by the heavy-atom method and refined by full-matrix least-squares techniques. The function minimized was $\Sigma w\Delta^2$ where $\Delta = ||F_o| - |F_c||$. Dispersion-corrected isolated atom form factors [14] were

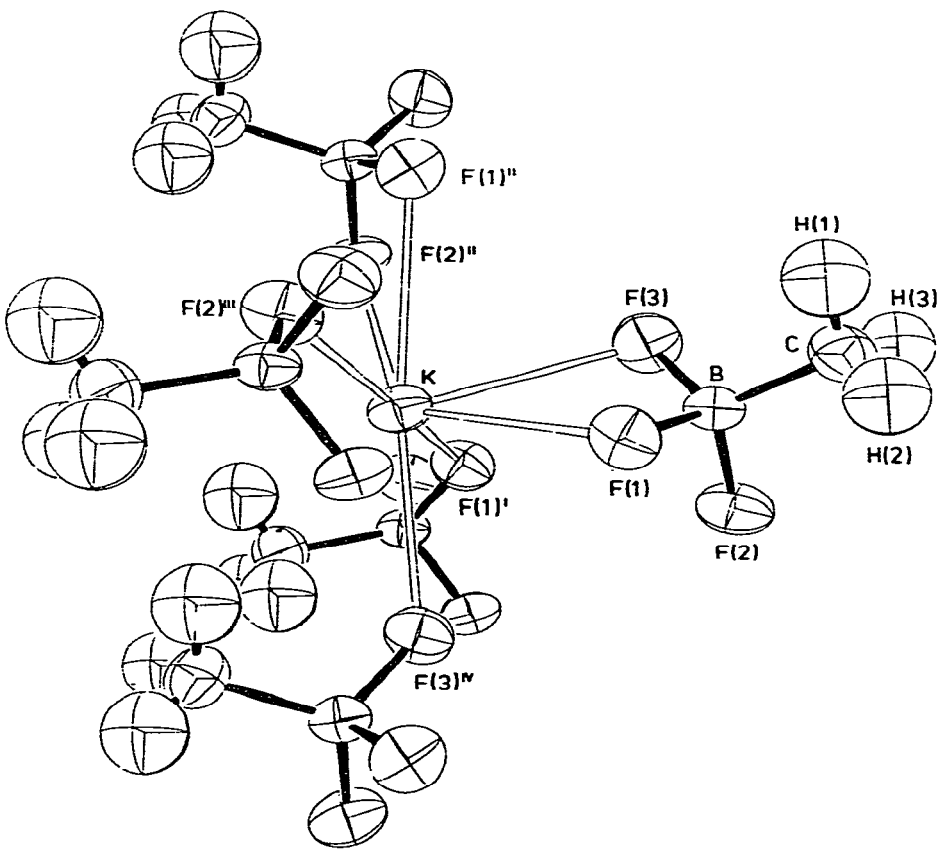

Fig. 1. Perspective drawing of the cation and five closest anions utilizing 50% probability thermal ellipsoids. Except for atoms in the asymmetric unit, only those involved in short K—F contacts are labeled.

TABLE 2

POSITIONAL AND THERMAL PARAMETERS [a] FOR $K[CH_3BF_3]$

Atom	x	y	z	U_{11} [b]	U_{22}	U_{33}	U_{12}	U_{13}	U_{23}
K	1691.8(2)	516.2(4)	1850.4(4)	546(2)	367(2)	326(2)	41(1)	28(2)	2(1)
B	3669(1)	279(2)	1783(2)	459(9)	299(7)	267(7)	−17(6)	−10(7)	10(6)
F(1)	3153.3(6)	−553(1)	3108(1)	595(6)	534(6)	345(5)	−64(4)	62(4)	101(4)
F(2)	3739.4(7)	−1083(1)	365(1)	760(8)	495(5)	343(5)	−87(5)	−3(5)	−125(4)
F(3)	3245.4(6)	1788(1)	997(2)	615(7)	415(5)	679(7)	39(4)	−80(5)	207(5)
C	4479(1)	867(3)	2620(3)	541(11)	548(10)	494(10)	−44(9)	−90(9)	−65(9)
H(1)	441(1)	189(4)	344(4)	88(8)					
H(2)	472(2)	−9(4)	322(4)	85(8)					
H(3)	482(1)	126(3)	168(3)	72(7)					

[a] For H X 10^3, otherwise X 10^4. [b] Form of the anisotropic and isotropic thermal ellipsoids is $\exp[-2\pi^2(h^2a^{*2}U_{11} + ... + 2hkb^*c^*U_{23})]$ and $\exp[-8\pi^2 U \sin^2\theta/\lambda^2]$ respectively.

used for all atoms except H (SDS). After three cycles employing anisotropic thermal ellipsoids for the nonhydrogen atoms, coordinates for the H atoms were taken from the three highest peaks (0.51—0.61 e $Å^{-3}$) in a difference Fourier synthesis. These atoms were subsequently refined isotropically. Then the absorption correction was applied, and further refinement including an extinction correction of the form $F_c = F_c^*(1 - \eta F_c^{*2}/\sin\theta)$ converged with $\eta = 3.2(4) \times 10^{-7}$, $R = \Sigma\Delta/\Sigma|F_0| = 0.026$ and $R_w = [\Sigma w\Delta^2/\Sigma w|F_0|^2]^{1/2} = 0.034$. For all reflections, the residuals are 0.046 and 0.036 respectively. In the final cycle the maximum magnitude of ζ/σ was 0.01. The flat plots of the function $\langle w\Delta^2\rangle$ versus $|F_0|$, $\sin\theta/\lambda$ and the indices atest to the validity of the weighting scheme. Densities in the final difference map range from 0.34 to —0.26 e $Å^{-3}$ and thus confirm the structure. Positional and thermal parameters are listed in Table 2, the numbering scheme being defined in Fig. 1. Distances and angles are given in Table 3. Calculations were made with SHELX-76, XANADU, ORTEP-2 and locally written programs. Tables of observed and calculated structure factors may be obtained from the authors.

Temperature factors U_{ij}^0 of the CBF_3 fragment were investigated for TLS rigid body motion [15]. The fit of the thermal parameters U_{ij}^c calculated by this twenty variable model to the U_{ij}^0's, as judged by the correspondence between $[\Sigma(U_{ij}^0 - U_{ij}^c)^2/10]^{1/2} = 11 \times 10^{-4}$ $Å^2$ and $[\Sigma\sigma^2(U_{ij}^0)/30]^{1/2} = 7 \times 10^{-4}$ $Å^2$, is excellent. Librational corrections to the B—C and B—F distances amount to 0.018 and 0.019 Å (mean), respectively. Unless specified to the contrary, uncorrected distances are referred to in this paper.

Description of the crystal structure

The structure confirms the ionic formulation for $K[CH_3BF_3]$. Since contacts between anions exceed the sums of the relevant van der Waals [16], the packing is apparently dictated by the cation-anion interactions. Indeed the cations form their closest contacts with F atoms in five anions, the midpoints of which roughly describe a square pyramid (Fig. 1). These polyhedra are linked perpendicular to *a* into layers with CH_3 groups occupying the surfaces. Seven K—F contacts are found at 2.678(1) to 2.965(1) Å. The next shortest (3.422(1) Å) exceeds the closest K—B distance (3.399(2) Å) and therefore is not considered to be bonding. For comparison, six K—F(B) contacts between 2.724(3) and 2.982(3) Å are found in $K[CF_3BF_3]$ [8] while ten such distances (2.758(3)—3.075(2) Å) were reported for KBF_4 [17]. The three shortest K—C distances (3.791(2)—3.924(2) Å) are distinctly longer than those in $K[Al(CH_3)_3CN]$ (3.24—3.65 Å) [18]. Apparently they as well as their concomitant K—H interactions (≥3.40 Å) contribute little to the stability of the crystals. This reluctance of the CH_3 group to participate in anion-cation interaction contrasts with the important contributions of K—F(CF_3) contacts to the crystal stability of $K[CF_3BF_3]$ [8].

The symmetry of the $CH_3BF_3^-$ anion is approximately C_{3v} with the CH_3 group staggered with respect to the BF_3 fragment. Small but significant deviations from this symmetry are shown by the F—B—F and C—B—F bond angles, the B—F bond distances and H—C—B—F torsion angles (Table 3). These undoubtedly result from packing effects. For instance, the longest B—F valency

TABLE 3

SELECTED GEOMETRICAL VALUES FOR $K[CH_3BF_3]$

Distances (Å)				
B—C	1.575(3)	1.593 [a]	K—F(1)	2.777(1)
			K—F(1)^{I} [c]	2.7182(9)
B—F(1)	1.434(2)	1.451 [a]	K—F(1)^{II}	2.965(1)
B—F(2)	1.418(2)	1.439 [a]	K—F(2)^{II}	2.759(1)
B—F(3)	1.420(2)	1.440 [a]	K—F(2)^{III}	2.678(1)
av. [b]	1.424(5)	1.443(4) [a]	K—F(3)	2.885(1)
			K—F(3)^{IV}	2.737(1)
C—H(1)	0.95(3)			
C—H(2)	0.91(3)			
C—H(3)	0.94(3)			
av.	0.93(2)			

Bond angles (°)			
C—B—F(1)	113.5(1)	B—C—H(1)	109(2)
C—B—F(2)	112.6(2)	B—C—H(2)	112(2)
C—B—F(3)	113.8(1)	B—C—H(3)	111(2)
av.	113.3(4)	av.	110.7(9)
F(1)—B—F(2)	104.5(1)	H(1)—C—H(2)	110(2)
F(1)—B—F(3)	105.5(1)	H(1)—C—H(3)	108(2)
F(2)—B—F(3)	106.1(1)	H(2)—C—H(3)	107(2)
av.	105.4(5)	av.	108.3(13)

Torsion angles (°) [d]					
F(1)—B—C—H(1)	−69(2)	F(1)—B—C—H(2)	53(2)	F(1)—B—C—H(3)	173(2)
F(2)—B—C—H(2)	−65(2)	F(2)—B—C—H(3)	54(2)	F(2)—B—C—H(1)	173(2)
F(3)—B—C—H(3)	−66(2)	F(3)—B—C—H(1)	52(2)	F(3)—B—C—H(2)	174(2)
av.	−67(1)		53(1)		173(1)

[a] Librationally corrected distances. [b] Errors in these average values are taken as the larger of $[\Sigma\sigma^2]^{1/2}/n$ and $[\Sigma(1-\bar{1})^2/n(n-1)]^{1/2}$. [c] Coordinates of primed atoms are related to those r in Table 2 as follows: $r^{I} = 0.5 - x, -y, z - 0.5$; $r^{II} = 0.5 - x, 0.5 + y, z$; $r^{III} = 0.5 - x, -y, 0.5 + z$; $r^{IV} = 0.5 - x, y - 0.5, z$. [d] A positive sign for the torsion angle ω (ABCD) indicates a clockwise rotation of BA into CD.

is that involving F(1), the only F atom entering more than two short K—F contacts. Since distortions found in the solid state are not large enough to indicate that the ideal symmetry would not be realized in a more symmetric medium, average geometric values (Table 3) will be considered in the following discussion.

The B—C bond length in $K[CH_3BF_3]$ is the shortest reported to date for a borate complex (Table 4). In particular, it is 0.059(8) and 0.050(7) Å shorter than those reported in the X-ray studies of $Li[B(CH_3)_4]$ [10] and $K[CF_3BF_3]$ [8], respectively. Indeed the B—C bond in $K[CH_3BF_3]$ comes close to that reported in the gas phase for trigonally coordinated $B(CH_3)_3$ [19], the librationally corrected distance in the borate being only 0.015(3) Å longer. This short valency is accompanied by the longest B—F distances reported for a fluoroborate (Table 4), small F—B—F bond angles (105.4(4)°) and concomitantly large C—B—F valence angles (113.3(4)°). Nearly tetrahedral F—B—F angles were found in $K[CF_3BF_3]$ [8] and $Cs[(CF_3)_2BF_2]$ [9] (Table 4). The geometry of the CH_3 group is normal for a X-ray determination, the B—C—H and H—C—H angles showing no significant deviations from the tetrahedral value.

TABLE 4

COMPARISONS OF SELECTED BORON COMPOUNDS

	B—C (Å)	f(B—C) $\times 10^2$ N m^{-1}	B—F (Å)	f(B—F) $\times 10^2$ N m^{-1}	F—B—F (°)	References
$Cs[(CF_3)_2BF_2]$	1.603(9) [a] 1.632(8) [b]	3.68	1.391(4)	4.17	108.1(4)	9
$K[CF_3BF_3]$	1.625(6)	3.63	1.391(5)	4.19	109.9(5)	8
$K[BF_4]$			1.386(3)	4.85	109.5(4)	17, 28
$K[CH_3BF_3]$	1.575(3)	3.70	1.424(5)	3.96	105.4(5)	this work
$Li[B(CH_3)_4]$	1.634(7)	3.40				10, 11
$B(CH_3)_3$	1.578(1)	3.84				19, 11

[a] CF_3 group staggered. [b] CF_3 group eclipsed.

Vibrational spectra

The IR and Raman spectra of $K[CH_3{}^{10}BF_3]$, $K[CH_3{}^{11}BF_3]$ and $K[CD_3BF_3]$ are collected in Table 5. The single crystal Raman spectrum of $K[CH_3BF_3]$ is shown in Fig. 2. Because of the poor solubility in H_2O, polarization measurements could be made only for the strongest Raman line associated with ν_3.

The relationship between the anion and the isoelectronic species CH_3CF_3

TABLE 5

VIBRATIONAL SPECTRA (cm^{-1}) OF $CH_3{}^{11}BF_3^-$, $CH_3{}^{10}BF_3^-$ AND $CD_3{}^{11}BF_3^-$

$CH_3{}^{11}BF_3^-$		$CH_3{}^{10}BF_3^-$		$CD_3{}^{11}BF_3^-$		Assignment
IR	Raman	IR	Raman	IR	Raman	
309vw	310w	310vw	311w	284vw	285w	ν_9 (e)
450vw 462vw	458w	451vw 463vw	459w	433vw 445vw	440w	ν_8 (e)
516m	517w	517m	518w	489m	491m	ν_2 (a_1)
				667s 673s	670sh	ν_{12} (e)
708m	708s	708m	708s	683m	683s	ν_3 (a_1)
				735vvw 743vvw		$CD_2H^{11}BF_3^-$
				770vvw		$\nu_2 + \nu_9$ (E)
781s 791s	786w	786s 796s	791w			ν_{12} (e)
				960vs		ν_7 (e)
				980vs	980vs	ν_5 (a_1)
				1018sh		$CD_2H^{11}BF_3^-$
1000sh 1022vs		1030sh 1050vs				ν_7 (e)
				1058w	1057m	ν_{11} (e)
				1116vw 1126vw		$CD_2H^{11}BF_3^-$
1091vs	1105vw	1129vs	1144vw			ν_1 (a_1)
				1156s 1186s	1155vw 1185vw	$\nu_1/\nu_2 + \nu_3$ (a_1)/(A_1)
				1205ms	1200vw	$CD_3{}^{10}BF_3^-$
1222vw		1223vw				$\nu_2 + \nu_3$ (A_1)
				1244vvw 1253vvw		$CD_2H^{11}BF_3^-$
1313s 1328vs 1334s		1317s 1332vs 1338s				ν_5 (a_1)
				1334vvw 1340vvw		$2\nu_{12}$ (A_1, E)
				1352vvw		$\nu_3 + \nu_{12}$ (E)
1440vvw	1449m	1441vvw	1450m			ν_{11} (e)
1494vvw		1498vvw				$\nu_3 + \nu_{12}$ (E)
1575vvw		1585vvw				$2\nu_{12}$ (A_1, E)
					2070m	ν_4 (a_1)
					2125m 2144m	$\nu_1 + \nu_5/\nu_2 + \nu_3 + \nu_5$ (A_1)
				2216m	2216m	ν_{10} (e)
2866vw	2851w	2868vw	2851w			$2\nu_{11}$ (A_1, E)
2925w	2925m	2925w	2925m			ν_4 (a_1)
				2936vvw		$CD_2H^{11}BF_3^-$
2956m 2964 m	2961m	2956m 2964m	2961m			ν_{10} (e)

TABLE 6

NOTATION, DESCRIPTION AND FREQUENCIES OF FUNDAMENTAL VIBRATIONS (cm^{-1})

			CH_3CF_3 [20]	$CH_3{}^{10}BF_3^-$	$CH_3{}^{11}BF_3^-$	CD_3CF_3 [20]	$CD_3{}^{11}BF_3^-$
a_1 (IR, Ra p)	ν_1	ν(BF,CF)	1280	1129	1091	1320	1156/1186
	ν_2	$\delta_s(BF_3,CF_3)$	604	517	516	570	489
	ν_3	ν(BC,CC)	828	708	708	796	683
	ν_4	ν(CH,CD)	2972	2925	2925	2168	2070
	ν_5	$\delta_s(CH_3,CD_3)$	1408	1332	1328	1068	980
a_2 (-,-)	ν_6	Torsion	220	200 [a]	200 [a]	162	144 [a]
e (IR, Ra dp)	ν_7	ν(BF,CF)	1220	1050	1022	1185	960
	ν_8	$\delta(BF_3,CF_3)$	544	459	458	524	440
	ν_9	δ(CBF,CCF)	371	310	309	340	284
	ν_{10}	ν(CH,CD)	3035	2960	2960	2280	2216
	ν_{11}	$\delta(CH_3,CD_3)$	1452	1450	1449	1046	1058
	ν_{12}	$\rho(CH_3,CD_3)$	965	791	786	811	670

[a] Calculated frequency.

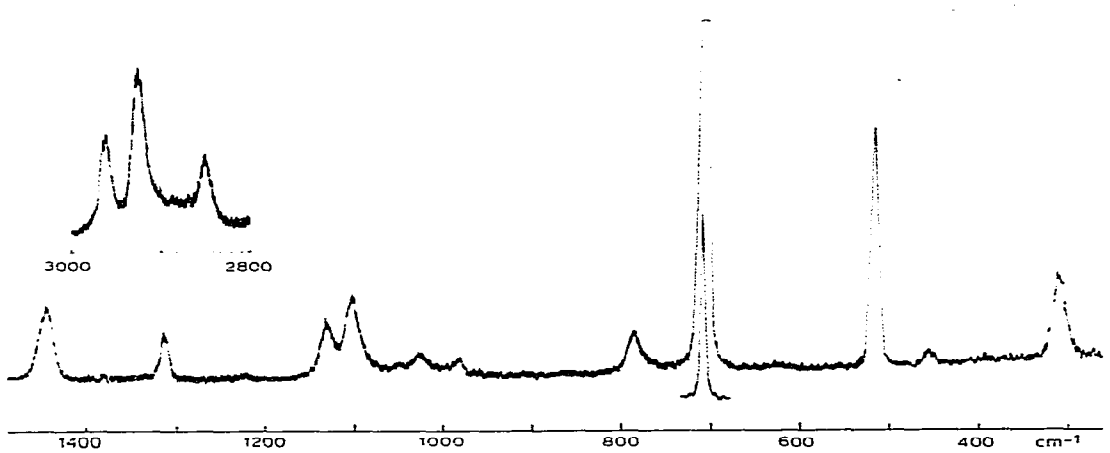

Fig. 2. Single crystal Raman spectrum of $K[CH_3BF_3]$.

and CD_3CF_3 [20] is a valuable key for the assignment of the spectra. Table 6 gives the description and notation of the fundamental vibrations ν_1 to ν_{12} for C_{3v} symmetry of the anion and emphasizes the analogy of CH_3CF_3 and CD_3CF_3 with $CH_3BF_3^-$ and $CD_3BF_3^-$. It may be noted that, in general, the vibrations of CH_3CF_3 and CD_3CF_3 are shifted towards the red in the anion; the exception of ν_7/ν_{11} of the deuterated species is only a formal one because here ν_7 and ν_{11} are coupled. The assignment is further supported by the $^{10}B/^{11}B$ shifts, which mainly affect the BF stretches ν_1 and ν_7, and by the results of the normal coordinate analysis given below. Except for the torsion ν_6 which is IR and Raman inactive, all the fundamentals were observed. The class e skeletal bends ν_8 and ν_9 are expected to be the lowest lying non-torsional fundamentals. As in CH_3CF_3, the a_1 vibrations ν_2 and ν_3 associated with the strongest Raman lines are mixed, and the descriptions given in Table 6 could also be exchanged. The choice between ν_1 and ν_7 is based on the intensities, while the symmetric CH_3 bending vibration ν_5 is expected to appear below ν_{11} whenever a methyl group is bound to a heavy or an electropositive element, and indeed a close analogy between $CH_3BF_3^-$ and CH_3Br [21] is revealed for all methyl vibrations. The

TABLE 7

INNER FORCE CONSTANTS (X 10^2 N m^{-1}), Scaled to 100 pm

(BC)	(1)	3.700	(1/2)	0.157	(2/2)	0.066	(3/3)	0.635
(CH)	(2)	4.835	(1/3)	0.319	(2/4) [b]	—0.041	(3/6) [b]	—0.212
(BF)	(3)	3.960	(1/4)	—0.043	(2/5) [a]	—0.020	(3/6) [a]	0.393
(HCH)	(4)	0.503	(1/5)	0.053	(2/5) [a]	0.104	(3/7) [a]	0.236
(BCH)	(5)	0.564	(1/6)	—0.136	(2/5) [b]	—0.124	(3/7) [b]	—0.304
(FBF)	(6)	1.411	(1/7)	0.119	(4/4)	—0.035	(6/6)	0.113
(CBF)	(7)	0.824	(5/7) [b]	0.098	(4/5) [a]	0.004	(6/7) [a]	0.024
Torsion	(8)	0.074	(5/7) [a]	—0.024	(4/5) [b]	0.032	(6/7) [b]	—0.059
					(5/5)	0.048	(7/7)	0.020

[a] Adjacent. [b] Opposite.

TABLE 8

CALCULATED FREQUENCIES (cm^{-1}) OF $CH_3{}^{11}BF_3^-$ (a), $CH_3{}^{10}BF_3^-$ (b) AND $CD_3{}^{11}BF_3^-$ (c) AND POTENTIAL ENERGY DISTRIBUTION 100 V_k, $V_k \geq 0.1$, IN TERMS OF INNER FORCE CONSTANTS

(a)/(b)/(c)	(BC)	(CH)	(BF)	(HCH)	(BCH)	(FBF)	(CBF)	(Torsion)
2926/2926/2098		98/ 98/ 98						
1340/1343/1171	16/19/66		/ /14	45/43/14	50/49/16	/ /13		
1092/1132/ 976	55/51/		31/30/25	/ /30	/ /33	24/24/14	11/11/	
708/ 708/ 683	18/18/13		52/52/44					
517/ 518/ 489	17/18/22					42/41/37	19/19/17	
200/ 200/ 144								100/100/100
2981/2981/2213		102/102/102						
1459/1460/1053				86/86/84				
1027/1051/ 959			55/62/97		50/44/18	11/13/19	13/14/17	
786/ 794/ 669			87/78/42		43/50/64	11/10/		
453/ 455/ 444						83/81/90		
310/ 310/ 283					14/14/23	14/14/	99/99/99	

increase of ν_1 upon deuteration is caused by crossing with ν_5, and furthermore anharmonic resonance of ν_1 with $\nu_2 + \nu_3$ affects the spectrum of the deuterated ^{11}B species, while the proximity of ν_1 and $\nu_2 + \nu_3$ required for resonance is not present for the ^{10}B analogue.

Normal coordinate analysis

A normal coordinate analysis based on idealized C_{3v} geometry with the averaged structural parameters of Table 3 was performed. An appropriate program [22] was used, and the starting inner force constants were taken from CH_3CF_3 [20] and $CF_3BF_3^-$ [8]. The force field was then refined, applying the constraints of a meaningful potential energy distribution, to reproduce the frequencies of the $CH_3{}^{10}BF_3^-$, $CH_3{}^{11}BF_3^-$ and $CD_3{}^{11}BF_3^-$ species. The CH stretch and bending vibrations were corrected by a factor of 1.01 to account for different anharmonicity of CH and CD modes. The final set of inner force constants is set out in Table 7, while Table 8 lists the calculated frequencies and their potential energy distribution in terms of inner force constants. The agreement between observed (Table 6) and calculated frequencies is satisfactory throughout; the isotopic shifts are well reproduced. The large value of the BC stretching force constant, 3.7×10^2 N m^{-1}, and the small BF stretching force constant, 3.96×10^2 N m^{-1}, are noteworthy.

Discussion

While the principal objective of this study was to clarify the CF_3/CH_3 substitution effect in the fluoroborates, it also yields previously unavailable information on F/CH_3 substitution in such compounds. The structural and force field information necessary for these comparisons is given in Table 4. Bond lengthening and decrease of the stretching force constant are correlated as expected. The substitutions CF_3/CH_3 and F/CH_3 result in comparable B—F bond lengthening and F—B—F angle contraction. Since analogous differences (0.021(2) Å and 2.6(2)° respectively) between CF_4 [23] and CH_3CF_3 [24] are only marginally smaller, the inductive effect may be invoked to explain them. The lengthening of the B—C bond in $Li[B(CH_3)_4]$ compared to $K[CH_3BF_3]$ may be rationalized similarly.

However, the inductive effect fails to explain why the B—C bond length in $K[CH_3BF_3]$ is shorter than that in $K[CF_3BF_3]$. The change in B—C length, 0.050(7) Å, is essentially identical with shortenings (0.050(6), 0.058(3) and 0.058(3) Å of M—CH_3 vs. M—CF_3 bonds, respectively, found for GeR_4 [1], SnR_4 [2] and PR_3 [3]. On the other hand, less shortening (0.025(2)Å) was observed for M=C [25], and such evidence has been cited in support of the electronegativity of M influencing the CF_3/CH_3 substitution effect [2,7,23,26].

For the borates, the shortening might imply that the resonance

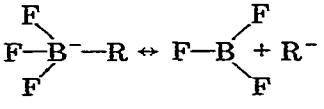

is more important for R = CF_3; that is, the B—CF_3 bond might be less covalent

than the B—CH_3 valence. Note that this does not depend on the substitution effect mentioned above.

More likely the charge distribution in RBF_3^- anions may be relevant here. CNDO calculations on related species [27] indicate that the B atom in RBF_3^- anions carries a positive charge. Since the C atom in $CF_3BF_3^-$ should be more positively charged than that in $CH_3BF_3^-$ (which may be negatively charged), differences in electrostatic force in these anions might well account for the different B—C bond lengths. Interestingly, the electrostatic contribution to the relatively long B—C interactions in the anion $B(CH_3)_4^-$ was calculated to be repulsive [27]. Clearly a quantification of the charge distribution in these compounds is a prerequisite for the separation of electrostatic and covalent contributions to the B—C bonding, and thus for a clearer understanding of the CH_3/CF_3 substitution effect.

Acknowledgement

Support by the Fonds der Chemie is gratefully acknowledged. We express our gratitude to Prof. C. Krüger, Mülheim, for making X-ray facilities available to us.

References

1 H. Oberhammer and R. Eujen, J. Mol. Struct., 51 (1979) 211.
2 R. Eujen, H. Bürger and H. Oberhammer, J. Mol. Struct., 71 (1981) 109.
3 H.J.M. Bowen, Trans. Faraday Soc., 50 (1954) 463.
4 D.J. Brauer, H. Bürger and R. Eujen, J. Organometal. Chem., 135 (1977) 281.
5 H. Oberhammer, J. Mol. Struct., 48 (1978) 389.
6 H. Günther, H. Oberhammer and R. Eujen, J. Mol. Struct., 64 (1980) 249.
7 H. Oberhammer, H. Günther, H. Bürger, F. Heyder and G. Pawelke, J. Phys. Chem., 86 (1982) 664.
8 D.J. Brauer, H. Bürger and G. Pawelke, Inorg. Chem., 16 (1977) 2305.
9 D.J. Brauer, H. Bürger and G. Pawelke, J. Organometal. Chem., 192 (1980) 305.
10 W.E. Rhine, G. Stucky and S.W. Peterson, J. Amer. Chem. Soc., 97 (1975) 6401.
11 H.J. Becher and F. Bramsiepe, Spectrochim. Acta, A, 35 (1979) 53.
12 A.B. Burg and J.R. Spielman, J. Amer. Chem. Soc., 83 (1961) 2667.
13 S.L. Stafford, Can. J. Chem., 41 (1963) 807.
14 J.A. Ibers and W.C. Hamilton (Eds.), International Tables for X-ray Crystallography, Vol. IV, The Kynoch Press, Birmingham, 1974, Table 2.3.1; J.A. Ibers and W.C. Hamilton (Eds.), ibid., Table 2.2B.
15 V. Schomaker and K.N. Trueblood, Acta Crystallogr., Sect. B, 24 (1968) 63.
16 A. Bondi, J. Phys. Chem., 68 (1964) 441.
17 G. Brunton, Acta Crystallogr., Sect. B, 25 (1969) 2161.
18 J.L. Atwood and R.E. Cannon, J. Organometal. Chem., 47 (1973) 321.
19 L.S. Bartell and B.L. Carroll, J. Chem. Phys., 42 (1965) 1135.
20 H. Bürger, H. Niepel and G. Pawelke, Spectrochim. Acta, A, 36 (1980) 7.
21 G. Graner, J. Mol. Spectrosc., 90 (1981) 394.
22 D. Christen, J. Mol. Struct., 48 (1978) 101.
23 V. Typke, M. Dakkouri and H. Oberhammer, J. Mol. Struct., 44 (1978) 85.
24 B. Beagley, M.O. Jones and M.A. Zanjanchi, J. Mol. Struct., 56 (1979) 215.
25 H. Oberhammer, J. Chem. Phys., 69 (1978) 468.
26 A. Yokozeki and S.H. Bauer, Top. Curr. Chem., 53 (1975) 71.
27 O. Gropen and A. Haaland, Acta Chem. Scand., 27 (1973) 521.
28 H.J. Becher, Colloq. Intern. CNRS, Paris, 191 (1970) 187.